Peter A. Rinck, MD • Helmut W. Fischer, MA[2] • Luce Vander Elst, PhD
• Yves Van Haverbeke, PhD • Robert N. Muller, PhD

Field-Cycling Relaxometry: Medical Applications[1]

Relaxometry between 10 kHz and 200 MHz (0.2 mT and 4.7 T) with a field-cycling device and a high-field-strength magnetic resonance (MR) unit permitted the determination of longitudinal relaxation rates of tissues and chemical compounds at numerous field strengths. The resulting nuclear magnetic relaxation dispersion profiles allowed the prediction of tissue contrast and efficacy of contrast agents at any field strength. Pure T1 contrast of normal brain tissue and pathologic lesions (multiple sclerosis, astrocytoma) increased from low field strengths to a maximum between 10 and 20 MHz and decreased afterward. Quadripolar dips reflecting the interaction between water and nitrogen atoms of the protein backbone appeared at 2.15 and 2.8 MHz, reducing T1 and opening the possibility of shorter imaging times and better tissue discrimination at these field strengths. Furthermore, it was shown that zero T1 contrast between normal and pathologic tissue samples may exist at certain field strengths. Gadolinium diethylenetriaminepentaacetic acid and gadolinium tetraazacyclododecanetetraacetic acid provided different contrast enhancement depending on the field strength.

Index terms: Brain, MR studies, 10.1214 • Brain neoplasms, MR studies, 10.363 • Magnetic resonance (MR), contrast enhancement • Magnetic resonance (MR), contrast media • Sclerosis, multiple, 10.871

Radiology 1988; 168:843–849

As magnetic resonance (MR) imaging and spectroscopy evolve as routinely used modalities in medicine, the use of MR relaxometry is increasing in research and clinical applications.

Relaxometry is the study of the behavior of nuclear relaxation processes dependent on internal and/or external parameters, among which are molecular and supramolecular structures, temperature, viscosity, pH, the influence of paramagnetic and ferromagnetic agents, and, last but not least, the magnetic field strength. For the latter application, relaxometry requires the use of a relaxometer, which produces dispersion curves of longitudinal relaxation rates (R1 = 1/T1) versus field strengths or frequencies at different temperatures. Principles and methods of field-cycling relaxometry have been described in detail (1,2), while to date biomedical applications have been rather limited (1–5).

It is well known that T1 in tissues is strongly dependent on field strength, while T2 is hardly influenced by alterations in field strength. Bottomley et al (4,6) and Escanye et al (7) proposed the prediction of T1 changes by empirical mathematical extrapolation between 1 and 100 MHz and 6 and 90 MHz, respectively. There is, however, no simple or absolute way to extrapolate further the T1 values of a complex system (like tissue) acquired at a certain field strength. T1 is determined by means of several factors, which depend on the tissue itself, and varies at different field strengths.

Comparison of contrast behavior in MR imaging at different field strengths performed with different MR imagers is very unsatisfactory because it is based on sporadic single measurements that do not allow any exact assessment or generalization. Furthermore, these calculations are complicated and time consuming. Often values are given at a single field strength or frequency, and even for these measurements, no protocols are established. Differences in gradient strength and pulse sequence can change these results significantly. In many instances, repetition of measurements leads to irreproducible data. We have commented on this earlier (8,9), and a recent publication concerning in vivo and in vitro T1 measurements of cerebrospinal fluid illustrates this problem once more (10). Thus, the approach to the contrast problem and imaging of pathologic conditions has been purely empiric (6,11–15). Deficiencies in measurement techniques have been due to the lack of a single reliable method. For exact answers, measurements of the same sample at different field strengths and with exactly the same variables are necessary. Field-cycling relaxometry aims to solve these problems.

Among our interests in MR relaxometry are tissue characterization and optimization of inherent contrast in MR imaging, as well as characterization of contrast agents, their design, and descriptions of their mechanisms of action. Two specific questions needed answers: To what extent, if any, is the inherent contrast dependent on field strength? To what extent, if any, is the behavior of contrast agents dependent on field strength?

An answer to the first question is necessary to evaluate the best experimental conditions (ie, pulse se-

[1] From the Department of Organic Chemistry and NMR Laboratory, State University at Mons, Medical Faculty, Belgium. From the 1987 RSNA annual meeting. Received October 1, 1987; revision requested January 9, 1988; revision received March 14; accepted April 25. P.A.R. was supported by grant no. RI 456/1-1 and 456/1-2 of Deutsche Forschungsgemeinschaft, Bonn, Federal Republic of Germany; H.W.F. was supported by grant no. ST2/0348 of the Commission of the European Communities, Brussels. The relaxometer was acquired through a grant of Fonds National de la Recherche Scientifique de Belgique. **Address reprint requests to** P.A.R., MR Center, University Hospital, N 7006 Trondheim, Norway.

[2] Current address: University of Bremen, Department of Physics, Federal Republic of Germany.

quences and pulse sequence values) for MR imaging at any field strength. In the long run, the aim is to collect data from a large population of well-defined normal and pathologic tissue samples, which will be stored in a data bank. An artificial intelligence system will then be able to select optimal values for imaging any suspected condition at any field strength.

The answer to the second question is essential for the proper design and use of contrast agents in MR imaging and spectroscopy. Their behavior might depend on field strength in a way that may lead to different indications according to the field strength (16).

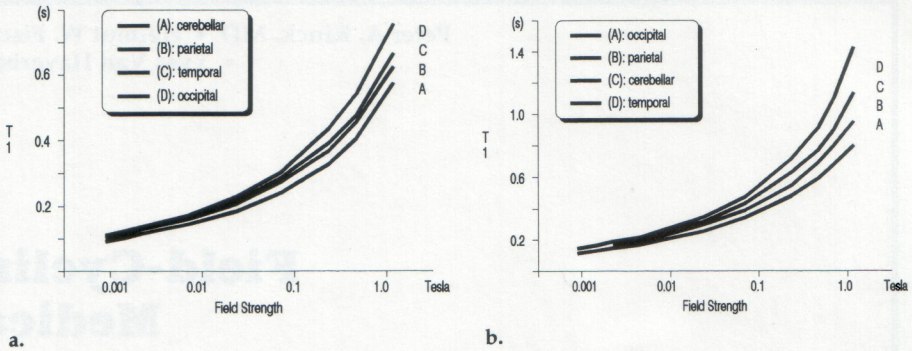

Figure 1. Graphs of the longitudinal relaxation times (T1) of white **(a)** and gray matter **(b)** of an adult brain.

MATERIALS AND METHODS

Proton nuclear magnetic relaxation dispersion (NMRD) profiles representing the relaxation rate 1/T1 versus the magnetic field strength were obtained with a research relaxometer (IBM, Yorktown Heights, New York). Measurements were obtained between 10 kHz (0.0002 T) and 50 MHz (1.2 T) with a standard spin-echo (SE) sequence (echo time [TE] = 6 msec) within 30–60 minutes. Relaxation rate profiles were obtained from six to 13 points. The T1 value at each frequency was calculated from 23 field-cycling sequences with the value of T_M, the measure time, the only value that was changed. Details of the system are given by Koenig and Brown (1).

T1 measurements at 200 MHz (4.69 T) were performed with inversion-recovery, Fourier transform on an MSL 200/15 system (Bruker Medizintechnik, Rheinstetten, Federal Republic of Germany). T2 values of the samples were determined with a Multispec system (Bruker Medizintechnik) with a Carr-Purcell-Meiboom-Gill sequence with a TE always shorter than 1 msec to minimize the effects of diffusion.

The sample size varied between approximately 50 and 500 mm^3. For proton density determination, the samples were weighed before the MR relaxometry examinations. After the experiments, they were dried in an oven for at least 7 days at 70°C and weighed again to estimate their water content.

Before the experiments, the best storage conditions had been determined, and a protocol was set up. Details on the protocol are available in a preliminary report (17). The final protocol will be published soon (18). In accordance with this protocol, relaxation times were examined of animal tissue and human brain samples of different locations either shortly after death or were flash frozen on dry ice, kept at −70°C, and defrosted shortly before the examinations. All examinations were performed at 37°C.

To our knowledge, flash freezing is a new efficient method for the preparation of samples that cannot be examined immediately. Flash frozen rat brain samples showed no significant changes in dispersion profiles compared with fresh samples. However, flash freezing of muscle tissue leads to characteristic slight changes (<10% change in dispersion rate), and with liver tissue there are great changes (>30% change in dispersion rates).

For the animal experiments, female Sprague-Dawley rats with an average weight of 250 g were used. Normal human tissue samples were obtained from two patients who had died of other than neurologic causes and who had no neurologic symptoms (man, 65 years old, accident victim; man, 60 years old, bronchial carcinoma). Five pairs of gray and white matter samples (frontal, parietal, temporal, occipital, cerebellar) from each patient were examined. In addition, between one and three samples per patient of the following regions were examined: thalamus and corpus callosum at different locations, putamen, claustrum, caudate nucleus, red nucleus, dentate nucleus, and pons. Pathologic samples included one large surgical specimen of a grade IV astrocytoma (man, 45 years old, right temporal tumor) and several small samples from a patient with proved multiple sclerosis (woman, 66 years old, multiple plaques).

Pure T1 contrast was calculated off-line with the following equation:

$$(T1_a - T1_b)/(T1_a + T1_b), \qquad (1)$$

where $T1_a$ and $T1_b$ represent the spin-lattice relaxation times of the two different tissues (19).

The theoretic contrast of SE sequences was calculated with Equation (1) in which T1 was replaced by I, the individual pixel or voxel intensity. I was calculated with the following equation:

$$I = A \times \rho \times K \times (1 - \exp^{-TR/T1}) \times \exp^{-TE/T2}, \qquad (2)$$

where A is a factor dependent on field strength representing the influence of the static magnetic field (B_0) on the signal-to-noise ratio (S/N), ρ is the water content of the brain, and K is a constant representing the contributions of flow and diffusion. K was considered as 1 and did not take into account any pulse imperfections.

For fast low-angle shot (FLASH) sequences, the following equation was used:

$$I = [A \times \rho \times K \times \sin\vartheta \times (1 - \exp^{-TR/T1}) \times \exp^{-TE/T2}]/[1 - \cos\vartheta \times \exp^{-TR/T1}], \qquad (3)$$

where A is a factor dependent on field strength representing the influence of the static magnetic field B_0 on the S/N, ϑ is the flip angle, ρ is the water content of the brain, and K is a constant representing the contributions of flow and diffusion (K = 1; modified after [20]). Again, to calculate the theoretic contrast, the resulting I replaces the respective T1 term in Equation (1).

RESULTS

Figure 1 depicts the relaxation times, T1, of white and gray matter of an adult. Both white and gray matter of different locations can be distinguished by means of different relaxation times due to the variable tissue composition.

The pure T1 contrast of gray and white matter in the brain has been calculated in Figure 2. In Figure 2a, additional results obtained at 200 MHz have been added. For clarification, only average values of temporal brain samples are shown in this figure. Cerebellar, frontal, parietal, and occipital samples had similar values and behavior. One of the most interesting observations was the increase of T1 contrast from low field strength to a peak at medium field strength, and a sharp decline afterward. This is also evident in Figure 2b and 2c: The pure T1 contrast between substantia nigra and neighboring white matter and dentate nucleus and neighboring cerebellar white matter climbs to a peak between 10 and 20 MHz and drops sharply afterward.

Similar results were observed in pathologic samples. Figure 3a shows the dispersion curves of a grade IV

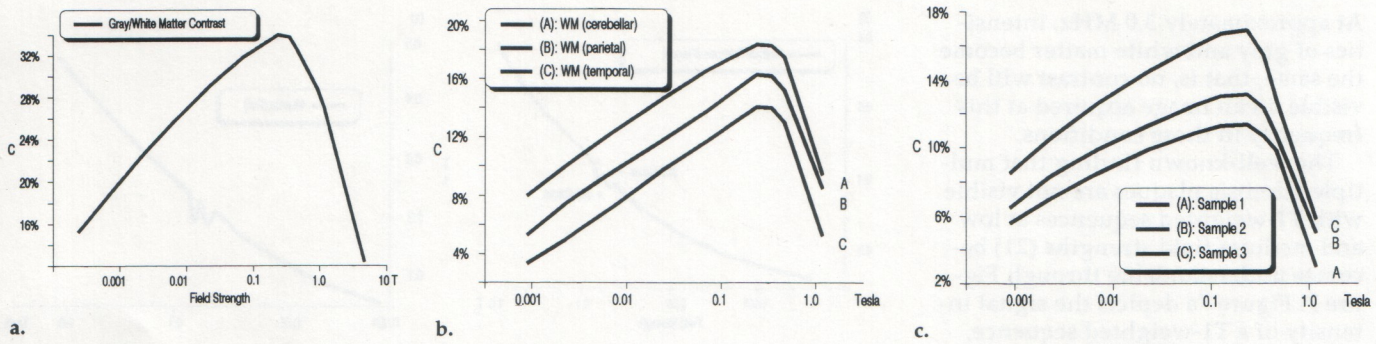

Figure 2. Graphs of pure T1 contrast (*C*) of gray and white matter of a human brain. **(a)** Graph shows additional results of the same sample obtained at 200 MHz added to data recorded with the field-cycling relaxometer. Pure T1 contrast increases from low field strength to a peak at medium field strength and declines sharply afterward. **(b, c)** Graphs depict the pure T1 contrast between substantia nigra and neighboring white matter **(b)** and dentate nucleus and neighboring cerebellar white matter **(c)** that again climbs to a peak between 10 and 20 MHz and drops afterward.

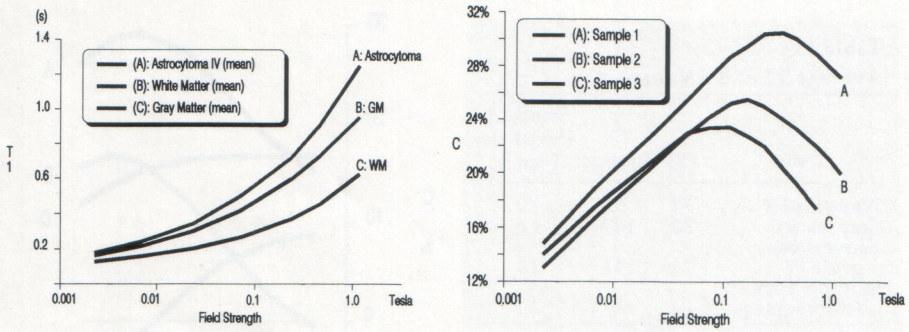

Figure 3. **(a)** Graph shows the dispersion curves of a grade IV astrocytoma compared with gray (*GM*) and white matter (*WM*) dispersion curves. The curves of gray matter and astrocytoma take a more or less parallel course, while white matter possesses higher relaxation times. **(b)** The pure T1 contrast curves between different parts of the astrocytoma versus white matter again reveal the peak at medium field strength.

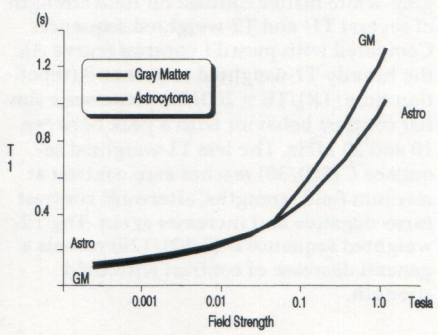

Figure 4. Longitudinal relaxation times of another sample of a grade IV astrocytoma (*Astro*) and gray matter (*GM*). In this case, the dispersion curves intersect in the low-field-strength range. At the point of intersection, no contrast exists between the two tissues. Note that at higher field strengths, the pathologic sample has a shorter T1 than that of gray matter.

astrocytoma compared with gray and white matter dispersion curves. The curves of gray matter and astrocytoma take a more or less parallel course, while white matter exhibits higher relaxation times. The pure T1 contrast curves between different parts of the astrocytoma versus white matter (Fig 3b) again reveal the peak at medium field strength.

All but two pairs of data, that is, those described in this article and numerous others, showed this contrast behavior. Contrast climbs to a maximum at approximately 20 MHz, where it reaches a peak between 20% and 30%. Earlier experiments with rat brain displayed the same behavior. The one exception was a contrast comparison between substantia nigra (the sample was inhomogeneous) and white matter. This contrast curve decays with field strength. The contrast between these two tissues, however, is irrelevant, because they are not adjacent tissues.

The relative error (standard deviation) of the T1 measurements (s_{T1}) was less than 2%. For similar T1 values, the absolute error of contrast (s_c) can be calculated with the following equation:

$$s_c = s_{T1}/(2^{1/2} \times T1), \qquad (4)$$

for $T1_a = T1_b$ and $s_{T1} = 2\%$, s_c is ±1.5%. Thus, the error bar would be ±1.5% for all samples and measurement points.

The second sample that did not possess the same properties is depicted in Figure 4. Here the dispersion curves of another sample of a grade IV astrocytoma and gray matter intersect in the low-field-strength range. At the point of intersection, no contrast exists between the two tissues.

The development of T1, however, is not as monotonic and smooth as shown with the previous measurements. If the resolution of the NMRD curve is increased, especially between 1.0 and 10.0 MHz, at least two dips can be detected. Figure 5a gives an example of T1 relaxation times of a multiple sclerosis sample, in which special attention was directed to the frequency range between 1.0 and 10.0 MHz. At approximately 2.1 and 2.8 MHz (0.05 and 0.066 T), two dips interrupt the otherwise steady increase of T1. Figure 5b gives a similar example for rat muscle in which the protein content is higher than that in average brain tissue.

The implications of relaxometric measurements on the choice of the most adequate pulse sequence for a particular indication are shown in Figures 6–9. Figure 6 shows the dependence on field strength of contrast between gray and white matter of several T1- and T2-weighted sequences. Compared with pure T1 contrast (curve A), the heavily T1-weighted sequence B has a similar contrast behavior, with a peak between 10 and 20 MHz. The less T1-weighted sequence C reaches zero contrast at medium field strengths; afterward, contrast inverts and increases again. The T2-weighted sequence D reveals a general decrease of contrast with field strength.

Figures 7a and 8a illustrate the signal intensities of normal gray and white matter and pathologic conditions in T1-weighted SE sequences.

At approximately 3.0 MHz, intensities of gray and white matter become the same; that is, no contrast will be visible on an image acquired at this frequency in these conditions.

The well-known finding that multiple sclerosis plaques are not visible with T1-weighted sequences at low and medium field strengths (21) becomes understandable through Figure 7. Figure 7a depicts the signal intensity of a T1-weighted sequence, showing a long interval at low and medium field strengths of poor or no contrast between multiple sclerosis plaques and white matter. Figure 7b illustrates the behavior of T2-weighted SE sequences with good contrast between gray matter, white matter, and multiple sclerosis plaques at low and medium field strengths.

Figure 8 presents a similar example for a high-grade astrocytoma, which, from MR imaging, is known to be difficult to see on T1-weighted images.

The signal intensity and contrast behavior of normal and pathologic brain tissue in fast imaging sequences is demonstrated in Figure 9. The peaks of the signal intensity curves move to lower flip angles with increasing field strength, and overall signal intensity decreases with field strength. Figure 9c depicts the contrast behavior between white matter and high-grade astrocytoma in FLASH sequences. It is obvious from these calculations that the proposed flip angle for brain imaging at 36° (22) only creates sufficient contrast between 1 and 10 MHz, whereas at 20 MHz, 36° offers zero contrast. At higher field strengths, contrast at this pulse angle is less than 5% and thus insufficient for the detection of pathologic changes.

Table 1 summarizes the ρ and T2 values of the samples mentioned above.

Although the influence of the magnetic field on paramagnetic relaxation is well documented (23), its effect is often neglected in the case of contrast media. Figure 10 shows the pivotal importance of the magnetic field. It depicts the dispersion curves of proton relaxation times of aqueous solutions of the two paramagnetic compounds gadolinium–diethylenetriaminepentaacetic acid (DTPA) and gadolinium tetraazacyclododecanetetraacetic acid (DOTA). It is obvious that the relaxation times of Gd-DOTA are shorter than those of Gd-DTPA at low field strength but slightly longer at high field strength. The relaxivity shown in this figure

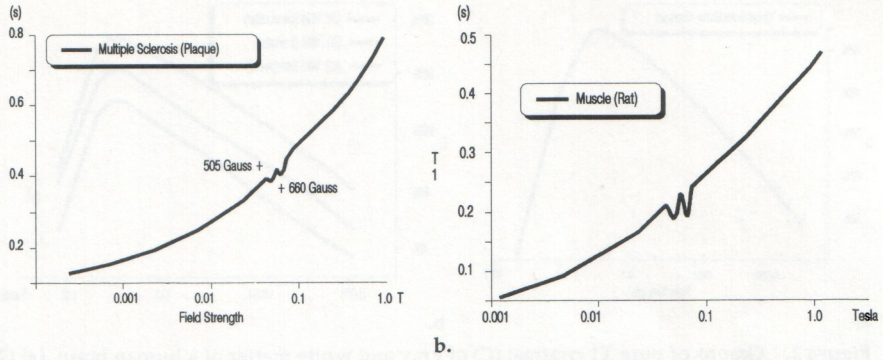

Figure 5. Graphs show that if the number of data points is increased, especially between 1.0 and 10.0 MHz, at least two dips in the T1 curves can be detected. **(a)** Graph gives an example of T1 relaxation times of a multiple sclerosis sample. At approximately 2.1 and 2.8 MHz (0.05 and 0.066 T), two dips interrupt the monotonic increase of T1. **(b)** Graph shows a similar example for rat muscle.

Table 1
Average T2 and ρ Values

Tissue	ρ (%)	T2 (msec)	Standard Deviation (msec)
White matter	72	89	1.2
Gray matter	82	105	1.6
Astrocytoma grade IV	78	144	2.2
Multiple sclerosis (chronic plaque)	84	140	2.1

(ie, the paramagnetic contribution of 1 mmol/L contrast agent to the relaxation rate of solvent protons) of Gd-DOTA is significantly higher than that of Gd-DTPA at low field strengths (16).

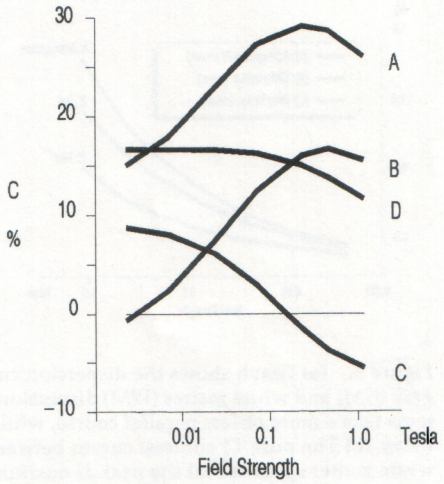

Figure 6. Graph shows dependence of gray-white matter contrast on field strength of several T1- and T2-weighted sequences. Compared with pure T1 contrast (curve *A*), the heavily T1-weighted sequence *B* (repetition time [TR]/TE = 200/30) possesses a similar contrast behavior with a peak between 10 and 20 MHz. The less T1-weighted sequence *C* (800/30) reaches zero contrast at medium field strengths; afterward contrast turns negative and increases again. The T2-weighted sequence *D* (2,000/120) reveals a general decrease of contrast with field strength.

DISCUSSION

Relaxometry will strongly influence the understanding of MR imaging and spectroscopy. The implications of its results will alter future experimental and commercial applications; in particular, the ability to predict tissue contrast is of paramount importance for the efficiency and efficacy of MR imaging.

The main factors influencing contrast in MR imaging are the relaxation times and, to a lesser extent, proton density. T2 is essentially independent of the magnetic field strength (6,23). Therefore, pure T2 contrast can be expected to stay the same at high and low field strengths.

T1 changes. However, the ratio between the NMRD profiles of normal gray and white matter, several nuclei of the brain, and all pathologic samples we examined varied with increasing field strength. In many cases, dispersion curves stay relatively close together at low and high field strengths and separate at medium field strengths (Figs 1–3), which leads to low or poor T1 contrast at low and high field strengths and to good contrast at medium field strengths, with a peak between 10 and 25 MHz (approximately 0.2 and 0.6 T). This underlines the validity of the findings by Escanye and collaborators (25) of a fast-growing tumor in mice (chemically induced rhabdomyosarcoma); they found the optimum contrast to be within the frequency range of 10–15 MHz.

Collections of relaxation data, such as the reviews by Bottomley et al (4,6), have shown a change of T1 re-

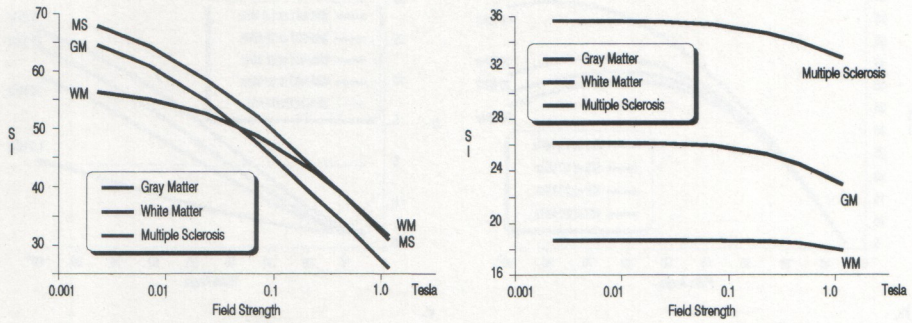

a. b.

Figure 7. Graphs illustrate the normal gray and white matter and pathologic signal intensity behavior (in arbitrary units) in T1-weighted SE sequences. At approximately 3.0 MHz, the signal intensities of gray and white matter become the same, that is, no contrast will be visible on an image acquired at this frequency. Multiple sclerosis plaques are not visible with T1-weighted sequences at high and medium field strengths. **(a)** Graph depicts the signal intensity behavior of a T1-weighted sequence (500/20), showing a long interval at low and medium field strengths of low or no contrast between multiple sclerosis plaques and white matter. **(b)** Graph shows the behavior of T2-weighted SE sequences (2,000/120) with good contrast between gray matter, white matter, and multiple sclerosis plaques at low and medium field strengths. *WM* = white matter, *MS* = multiple sclerosis, *GM* = gray matter.

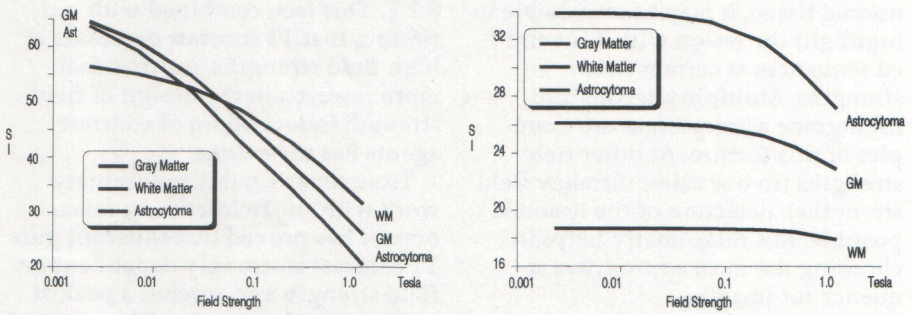

a. b.

Figure 8. Graphs show the dependence of signal intensity (in arbitrary units) on field strength for a high-grade astrocytoma, which is known to be difficult to detect on T1-weighted images. Data obtained with SE sequences of 500/20 **(a)** and 2,000/120 **(b).** *WM* = white matter, *GM* = gray matter.

laxation of tissues with field strength, but they cannot be compared with data acquired from identical samples under identical experimental conditions in a single MR device. It is understood that there are always errors associated with relaxation time measurements of tissues. Any volume of normal and pathologic tissue may contain different tissue components that will contribute to the MR signal. The advantages of our relaxometric measurements are the selection of tissue that looks homogeneous and the ability to reject mixed tissue samples. This is impossible in MR imaging in which relaxation time measurements are usually obtained from only two or three images taken at different time delays and are additionally hampered by partial volume effects. A number of other factors deteriorate the quality of in vivo measurements. Diffusion, perfusion, flow within the partial volume, artifacts, and interindividual variations in the delineation of regions of interest add to the uncertainty of direct in vivo measurements.

Because T1 relaxation time values are absolute time values, noise has not been considered in the pure T1 contrast determination (26–29). Theory and experimental data concerning the S/N dependence versus magnetic field strength support the idea of an optimal clinical imaging field in the 0.2–0.6-T range. Hart and collaborators found a general trend for the T1 contrast-to-noise ratio to increase with field strength throughout the range of field strengths used for imaging (26). They stated, however, that the data they presented were very limited and did not necessarily indicate how well a particular diseased tissue will be discriminated relative to its host tissue in clinical imaging. They claimed that more data were needed. It is clear that these additional data could easily be collected with our field-cycling system.

Hoult et al (27) underlined in a 1986 paper that the S/N immediately following a 90° pulse increases linearly at low and medium field strengths and flattens out at higher field strengths, resulting in diminishing gains as the field strength is increased. This limits their earlier statement claiming a linear relationship between the S/N and field strength, which is only true for MR spectroscopy (30). The dependencies described in the 1979 paper (30) are presumably inaccurate because the resistivities of the various tissues within the human body are decreasing with increasing frequency.

With increasing field strength, less and less molecular motion contributes to relaxation processes, and the T1 relaxation time of tissues approaches that of pure water. Thus, for T1, the higher the field strength, the more the human body looks like a water bottle. The water content of tissues, however, is neither tissue nor lesion specific but rather is changed by multiple factors. At lower field strengths, there is a stronger multifactorial dependence of T1 on total water content, macro- and microscopic water distribution, and interactions between macromolecules and water. Thus, theoretically it is more difficult to create physiologically relevant T1 contrast at high field strengths than at low field strengths (31). Our results proved that pure T1 contrast deteriorates at high field strengths. On the other hand, they show a decline of contrast at low and ultralow field strengths. This disagrees with earlier theories (20,31).

The question of optimal clinical field strength is an area of much debate and has important commercial implications. Data obtained with field-cycling relaxometry may not adequately describe the clinical situation, but the findings concerning contrast combined with the earlier results by Hoult et al concerning signal strength and noise (27,30) underline the arguments supporting the use of low and medium field strengths for head and body imaging. High field strengths may be ideal for spectroscopy and head-only imaging.

The T1 of tissues does not show a monotonic increase with field strength but reveals at least two dips (quadrupolar dips) around 2.1 and 2.8 MHz. Because the dips reflect interactions between water protons and nitrogen atoms of the protein backbone of cells (5,32), they are more marked in muscle tissue (in our case, approximately 20%) but are seen well in brain tissue (in our multiple sclerosis sample, approximately 7.5%)

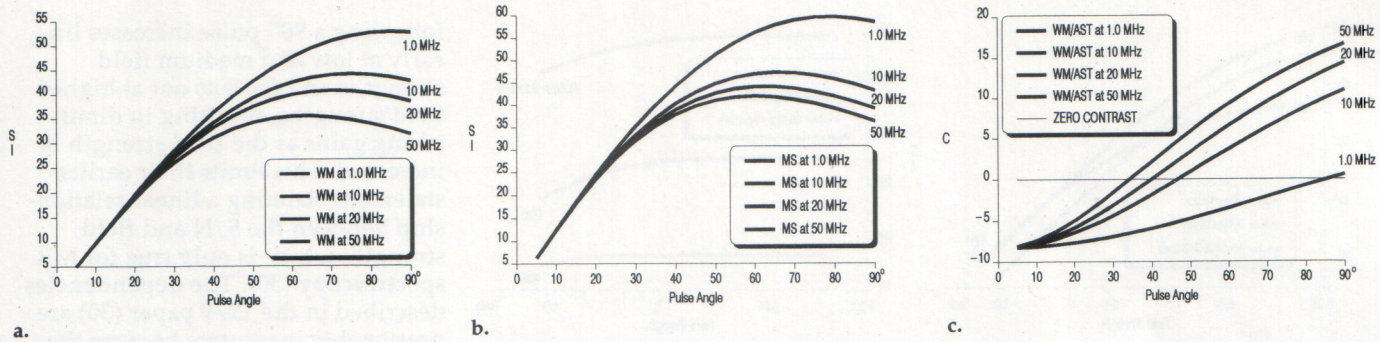

Figure 9. Diagrams show signal intensity (in arbitrary units) and contrast behavior of white matter **(a)** and multiple sclerosis plaques **(b)** with FLASH sequences. The peaks of the signal intensity curves move to lower flip angles with increasing field strength, and overall signal intensity decreases with field strength. **(c)** Diagram depicts the contrast (in percent) behavior between white matter and high-grade astrocytoma in FLASH sequences. All data were obtained at 500/20.

and may be exploited for ultralow-field-strength imaging. This may allow better tissue discrimination. On the other hand, the shorter T1 and subsequent gain in S/N at these frequencies allow a reduction of data acquisition time and thus imaging time.

Damadian in 1971 (33) and others shortly afterward (14,34) found that neoplastic tissue generally has an elevated T1 (shorter 1/T1) compared with normal tissue. This finding created the philosophy of the possibility of distinguishing between normal and abnormal tissues with relaxation time values. Relaxation rate profiles reported here and profiles of human breast cancer and normal human breast tissue published earlier by Koenig et al (35) prove that this hypothesis is only partially true and should not be generalized. At certain field strengths, pathologic tissue may have a lower T1 than normal tissue. This observation holds for neoplastic and nonneoplastic diseased states and also influences contrast. MR images obtained before the crossing point of the two signal intensity versus field strength curves will show a positive contrast compared with a negative contrast at higher field strengths. There is no T1 contrast at the field strength of the intersection. This means that comparison of two images taken at two different field strengths may create difficulties in the assessment of a disease (36).

This is even more marked with T1-weighted sequences. Although it was known from imaging experience that certain pathologic conditions could be seen at one field strength but not at another (37,38), the origin and implications of the phenomenon are only visible with MR relaxometry. It proves that even a complete reversal of contrast from positive to negative between low and high field strengths is possible. In T1-weighted sequences, this feature can be intensified by the influence of T2 and proton density. Even if the T1 of a diseased tissue is higher than that of normal tissue, it may be impossible to highlight the lesion with T1-weighted sequences at certain field strengths. Multiple sclerosis and high-grade astrocytomas are examples of this feature. At other field strengths (in our cases, ultralow field strengths), detection of the lesion is possible. MR relaxometry helps in choosing the most appropriate sequence for imaging.

The same holds true for fast imaging sequences. Here, the contrast for every indication has to be precalculated, to select the best pulse angle (Fig 9). The claim that contrast media should be used in any case with these sequences results from the ignorance of this problem, as was the case with SE sequences some years ago (39). In many cases, precalculation of contrast in multiple SE sequences allows the differentiation of pathologic conditions without contrast agents (8,9, 40,41).

Paramagnetic contrast agents cause a relatively strong decrease in T1 and, to a lesser extent, in T2. Commonly used agents are transition metals and lanthanides bound in complexes with various polydentate chelate ligands, such as Gd-DTPA and Gd-DOTA (42). Similar considerations as those mentioned are true for these agents, too. They possess a relaxivity that changes with the field strength. Furthermore, it is sometimes underestimated and underappreciated that the efficiency of contrast agents is highly dependent on the field strength (16,43,44). For instance, Gd-DOTA becomes more efficient as a contrast agent than Gd-DTPA at field strengths lower than 0.2 T. Therefore, the use of Gd-DOTA would give better results at low field strengths than at high field strengths. It remains true, however, that both substances lose their efficiency at field strengths higher than 0.2 T. This fact, combined with our finding that T1 contrast decreases at high field strengths, justifies that more research in the design of field strength independent of contrast agents has to be done.

To summarize, this preliminary work with the field-cycling relaxometer has proved that inherent pure T1 contrast is strongly dependent on field strength and reaches a peak at medium field strengths. T1-weighted contrast in some cases can disappear at certain field strengths, and T2-weighted contrast decreases with field strength. The T1 of lesions is not always higher than the T1 of normal tissue but might be lower. Finally, the efficiency of paramagnetic contrast agents dependent on field strength must not be overlooked, to achieve the best conditions for clinical utilization of the method. ■

Acknowledgments: The authors thank Armand Lowenthal, MD, and Denise Karcher, MD, for providing the normal and pathologic brain samples, and Alain Roch, MA, for relaxation time measurements at 200 MHz.

References

1. Koenig SH, Brown III RD. Relaxometry of tissue. In: Gupta RK, ed. NMR spectroscopy of cells and organisms. Boca Raton, Fla: CRC, 1988 .
2. Koenig SH, Brown III RD. The importance of the motion of water in biomedical NMR. In: Petersen SB, Muller RN, Rinck PA, eds. An introduction to biomedical nuclear magnetic resonance. New York: Thieme, 1985; 50–58.
3. Beaulieu CF, Clark JI, Brown III RD, Spiller M, Koenig SH. Magnetic field dependence of 1/T1 in calf lens cytoplasm in vitro: solvent-protein cross relaxation. In: Book of abstracts: Society of Magnetic Resonance in Medicine 1987. Vol. 2. Berkeley, Calif: Society of Magnetic Resonance in Medicine, 1987; 598.

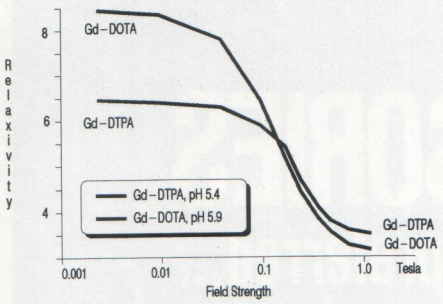

Figure 10. Diagram shows the relaxivities (in 1/sec·mmol) of aqueous solutions of Gd-DTPA and Gd-DOTA. It is obvious that the relaxivity of Gd-DOTA is higher than that of Gd-DTPA at low field strengths but slightly lower at high field strengths.

4. Bottomley PA, Hardy CJ, Argersinger RE, Allen-Moore G. A review of ^{1}H nuclear magnetic resonance relaxation in pathology: are T1 and T2 diagnostic? Med Phys 1987; 14:1–37.
5. Winter F, Kimmich R. NMR field cycling spectroscopy of bovine serum albumin, muscle tissue, micrococcus luteus, and yeast: $^{14}N^{1}H$ quadrupole dips. Biochim Biophys Acta 1982; 719:292–298.
6. Bottomley PA, Foster TH, Argersinger RE, Pfeifer LM. A review of normal tissue hydrogen NMR relaxation times and relaxation mechanisms from 1–100 MHz: dependence on tissue type, NMR frequency, temperature, species, excision, and age. Med Phys 1984; 11:425–448.
7. Escanye JM, Canet D, Robert J. Frequency dependence of water proton longitudinal nuclear magnetic relaxation times in mouse tissues at 20°C. Biochim Biophys Acta 1982; 721:305–311.
8. Rinck PA, Meindl S, Higer HP, Bieler EU, Plannenstiel P. Brain tumors: detection and typing by use of CPMG sequences and in vivo T2 measurements. Radiology 1985; 157:103–106.
9. Rinck PA, Appel B, Moens E. Relaxationszeitmessung der weissen und grauen substanz bei patienten mit multipler sklerose. ROFO 1987; 147:661–663.
10. Condon B, Patterson J, Jenkins A, et al. MR relaxation times of cerebrospinal fluid. J Comput Assist Tomogr 1987; 11:203–207.
11. Bottomley PA, Hardy CJ, Argersinger RE. The field dependence of T1 contrast between normal and pathologic tissue: a review. In: Book of abstracts: Society of Magnetic Resonance in Medicine 1986. Vol. 2. Berkeley, Calif: Society of Magnetic Resonance in Medicine, 1986; 407–408.
12. Fullerton GD, Cameron IL, Ord VA. Frequency dependence of magnetic resonance spin-lattice relaxation of protons in biological materials. Radiology 1984; 151:135–138.
13. Hopkins AL, Yeung HN, Bratton CB. Multiple field strength in vivo T1 and T2 for cerebrospinal fluid protons. Magn Reson Med 1986; 3:303–311.
14. Inch WR, McCredie JA, Knispel RR, Thompson RT, Pintar MM. Water content and proton spin relaxation time for neoplastic and non-neoplastic tissues from mice and humans. JNCI 1974; 52:353–356.
15. Johnson CA, Herikens RJ, Brown MA. Tissue relaxation time: in vivo field dependence. Radiology 1985; 156:805–810.
16. Muller RN, Vander Elst L, Rinck PA, et al. The importance of nuclear magnetic relaxation dispersion (NMRD) profiles in MRI contrast media development. Invest Radiol (in press).
17. Fischer H, Muller RN, Rinck PA, Vander Elst L, Van Haverbeke Y. Variation of T1 of rat tissues with storage conditions measured over a wide frequency range. In: Proceedings of the fifth annual meeting of the European Workshop on Nuclear Magnetic Resonance in Medicine, 1987; 20–21.
18. Fischer H, Van Haverbeke Y, Rinck PA, Schmitz-Feuerhake I, Muller RN. The effect of aging and storage conditions on excised tissues as monitored by longitudinal relaxation dispersion profiles of tissues: dependence of 1/T1 of storage conditions (forthcoming).
19. American College of Radiology. Glossary of NMR terms. In: Petersen SB, Muller RN, Rinck PA, eds. An introduction to biomedical nuclear magnetic resonance. New York: Thieme, 1985; 178–190.
20. Crooks LE, Arakawa M, Hoenninger J, McCarten B, Watts J, Kaufman L. Magnetic resonance imaging: effects of magnetic field strength. Radiology 1984; 151:127–133.
21. Appel B, Moens E, Rinck PA, Lowenthal A. MRI approach of multiple sclerosis: about 449 cases examined at 0.15 T. J Neuroradiology (in press).
22. Mills TC, Ortendahl DA, Hylton NM, Crooks LE, Carlson JW, Kaufman L. Partial flip angle imaging. Radiology 1987; 162:531–539.
23. Bertini I, Lucinat C. NMR of paramagnetic molecules in biological systems. Menlo Park, Calif: Cummings, 1986.
24. Beall MT, Amtey SR, Kasturi SR. Data handbook for biomedical applications. New York: Pergamon, 1984; 56–67.
25. Escanye JM, Canet D, Robert J, Brondeau J. NMR proton longitudinal relaxation times in tissues of tumor-bearing C3H mouse studied as a function of frequency. Cancer Detect Prev 1981; 4:261–265.
26. Hart HR, Bottomley PA, Edelstein WA, et al. Nuclear magnetic resonance imaging: contrast-to-noise ratio as a function of strength of magnetic field. AJR 1983; 141:1195–1201.
27. Hoult DI, Chen C-N, Sank VJ. The field dependence of NMR imaging. II. Arguments concerning optimal field strength. Magn Reson Med 1986; 3:730–746.
28. Wehrli FW, Herfkens RJ, MacFall JR, Shutts D. Contrast and contrast-to-noise in magnetic resonance imaging. In: Petersen SB, Muller RN, Rinck PA, eds. An introduction to biomedical nuclear magnetic resonance. New York: Thieme, 1985; 59–67.
29. Young IR. Considerations affecting signal and contrast in NMR imaging. Br Med Bull 1984; 2:139–147.
30. Hoult DI, Lauterbur PC. The sensitivity of the zeugmatographic experiment involving human subjects. J Magn Reson 1979; 34:425–433.
31. Eastwood L. Proton density, T1 and T2: computed images. In: Petersen SB, Muller RN, Rinck PA, eds. An introduction to biomedical nuclear magnetic resonance. New York: Thieme, 1985; 40–49.
32. Kimmich R, Nusser W, Winter F. In vivo NMR field-cycling relaxation spectroscopy reveals $^{14}N^{1}H$ relaxation sinks in the backbones of protein. Phys Med Biol 1984; 29:593–596.
33. Damadian R. Tumor detection by nuclear magnetic resonance. Science 1971; 171: 1151–1153.
34. Hazelwood CF, Cleveland G, Medina D. Relationship between hydration and proton nuclear magnetic resonance relaxation times in tissues of tumor-bearing and non-tumor-bearing mice: implications for cancer detection. JNCI 1974; 52:849–853.
35. Koenig SH, Brown III RD, Adams D, Emerson D, Harrision CG. Magnetic field dependence of 1/T1 of protons in tissue. Invest Radiol 1984; 19:76–81.
36. Rinck PA, Muller RN, Fischer HW. Feld- und temperaturabhängigkeit des kontrastes in der magnetresonanz-bildgebung. ROFO 1987; 2:200–206.
37. Sipponen JT, Sepponen RE, Tanttu JI, Sivula A. Intracranial hematoma studied by MR imaging at 0.17 and 0.02 T. J Comput Assist Tomogr 1985; 4:698–704.
38. Smith FW, Cherryman GR, Steyn JH. A comparison of T1 measurements at 1.7 and 3.4 MHz in the diagnosis of prostatic carcinoma. Magn Reson Med 1985; 2:350–354.
39. Rinck PA, Bielke G, Meves M. Modified spin echo sequence in tumor diagnosis. Magn Reson Med 1984; 1:237.
40. Rinck PA, Muller RN, Harms SE. Kontrast in der magnetresonanz-bildgebung. Radiol Diagn (Berlin) 1987; 28:151–167.
41. Ziedses des Plantes BG, Falke TMH, den Boer JA. Pulse sequences and contrast in magnetic resonance imaging. RadioGraphics 1984; 6:869–883.
42. Brasch RC. An overview of contrast agents for magnetic resonance imaging. In: Runge VM, Claussen C, Felix R, James AE, eds. Contrast agents in magnetic resonance imaging. Princeton, NJ: Excerpta Medica, 1986; 11–13.
43. Geraldes CFGC, Sherry AD, Brown III RD, Koenig SH. Magnetic field dependence of solvent proton relaxation rates induced by Gd^{3+} and Mn^{2+} complexes of various polyaza macrocyclic ligands: implications for NMR imaging. Magn Reson Med 1986; 3:242–250.
44. Lauffer RB, Brady TJ, Brown III RD, Baglin C, Koenig SH. 1/T1 NMRD profiles of solutions of Mn^{2+} and Gd^{3+} protein chelate conjugates. Magn Reson Med 1986; 3:541–548.